Solar Energy Materials & Solar Cells 128 (2014) 41–47

Contents lists available at ScienceDirect

Solar Energy Materials & Solar Cells

journal homepage: www.elsevier.com/locate/solmat

The stability of normal vs. inverted organic solar cells under highly damp conditions: Comparison with the same interfacial layers

Donggeon Han, Seunghyup Yoo *

Department of Electrical Engineering, Korea Advanced Institute of Science and Technology (KAIST), 291 Daehak-ro (373-1 Guseong-dong), Yuseong-gu, Daejeon 305–701, Republic of Korea

ARTICLE INFO

Article history:
Received 22 February 2014
Received in revised form
24 April 2014
Accepted 27 April 2014
Available online 29 May 2014

Keywords:
Organic solar cells
Stability
Lifetime
Inverted solar cells

ABSTRACT

The stability of normal and inverted organic solar cells is investigated under a highly damp condition (90% relative humidity) in air. For fair comparison, both cells are fabricated not only with the same active layers but also with the same interfacial and electrode layers. The experimental results indicate that the inverted cells do outlive the normal cells and that the top electrode/interfacial layer is a vulnerable component that affects the life time most significantly. Furthermore, inverted cells are shown to have a degradation trend that differs significantly from that of the normal cells: the former have a voltage-dominant degradation due to the change in the work function of the metal oxide-based anodic interfacial layers; and the latter have a current-dominant degradation associated with the formation of bubble-like features. Based on the causes of degradation, methods for avoiding or delaying the observed degradations are proposed and tested for each type of cells. 28 (1.4) fold enhancement in T_{80}-lifetime is achieved for inverted (normal) cells with the proposed method.

1. Introduction

Organic solar cells (OSCs) are next-generation photovoltaic devices that have garnered significant interest for a potential use in diverse applications. The power conversion efficiency of OSCs has soared over the past few years and has reached up to 12%, which is a value that can be considered sufficiently large to merit commercial-scale production [1]. However, the most troublesome aspect of deploying OSCs in real-world applications is their uncertain device stability [2–4]. Typically, the organic semiconductors used in OSCs are subject to degradation upon exposure to ambient air. Furthermore, low work-function metals, which are often used as cathodes in OSCs, are also known to be susceptible to ambient conditions. In order to overcome such inherent problems related to the low work-function cathodes, inverted-architecture OSCs ('inverted OSCs' hereafter) have been proposed where the cathode is located underneath the organic and anode layers [5]. In several previous studies, inverted OSCs have exhibited significantly better stability than the conventional architecture OSCs ('normal OSCs' hereafter) [6–8]. However, the layers in the normal and inverted OSCs investigated in those studies often consisted of different electrodes or interfacial layers; for example, Ca/Al or LiF/Al was used as the top cathode for the control cells in the conventional architecture while ITO coated with a TiO_x or ZnO layer was used as the bottom cathode for the inverted architecture. These differences could be acceptable for a quick demonstration of the potential superior stability of inverted OSCs; however, such experiments may not provide a fair comparison, thus failing to demonstrate the full benefits and being subject to overestimation or exaggeration due to the reactive natures of Ca/Al and LiF/Al.

In this study, normal and inverted OSCs are fabricated with all participating layers using the same materials in an effort to determine whether one architecture is truly better than the other and, if so, why and by how much it is better. In particular, the OSCs' stability against humid ambient air is compared in accelerated testing conditions (relative humidity (RH) of 90%) as they are prone to degrade rapidly when exposed to excessive humidity [9]. Investigating the evolution of cell performance in damp conditions is meaningful because (i) the long-term effects of moisture on OSCs can be easily predicted; (ii) the OSC endurance can be estimated for extreme wet conditions, which are known to occur, for example, in overseas shipping environments [10]; and (iii) the basic data needed to estimate the protection requirements for OSCs from humidity can be provided for target operation times under given average weather conditions.

* Corresponding author. Tel.: +82 42 350 3483; fax: +82 42 8083.
E-mail addresses: syoo@ee.kaist.ac.kr, syoo@ee.kaist.ac.kr (S. Yoo).

http://dx.doi.org/10.1016/j.solmat.2014.04.036
0927-0248/

2. Experimental

In order to fairly compare the stability of normal and inverted OSCs, both cells were fabricated using the same interfacial layers (MoO_x for the anodic buffer layer and TiO_x for the cathodic buffer layer) and the same electrodes (ITO as bottom electrode and Al as top electrodes) as shown in Fig. 1(a) and (b). The stability of these devices under damp conditions was monitored in the sequence summarized in Fig. 1(c). Before each evaluation, the cells were illuminated with an AM 1.5G light source for 7.5 ± 2.5 min. This process is known as "light soaking" and is necessary for proper operation of the inverted OSCs that include buffer layers of ZnO and TiO_x [11,12]. After a given time for 'aging' inside an environmental chamber (TH-PE-025, JEIO Tech, Korea) held at an RH of 90% and temperature of 27 °C (condition close to ISOS-D-3 [13], with humidity slightly more severe and temperature maintained around room temperature), the devices were examined under a microscope for microscopic or visual abnormalities.

TiO_x solution was prepared as follows [14]. Titanium(IV) isopropoxide (5 ml), 2-methoxyethanol (20 ml), and ethanol amine (2 ml) were injected in sequence into a three-neck flask connected with a water condenser and nitrogen gas inlet/outlet; then, the solution was stirred at room temperature for 1 h. Afterward, the solution was heated and stirred at 80 °C for 1 h, followed by heating to 120 °C and stirring for 1 h. After cooling to room temperature, 10 ml of methanol was injected into the solution. The TiO_x solution was prepared through diluting the TiO_x precursor in methanol with a ratio of 1:200 by weight.

Substrates were cleaned in an ultrasonic bath using soapy water, DI–water, acetone, and isopropanol in sequence and dried in a vacuum oven. The substrates were plasma-cleaned (PDC-32G, Harrick Plasma) before MoO_x (Alfa Aesar, 99.9995%) thermal evaporation or TiO_x spin-cast. TiO_x was spin-cast at 2500 rpm for 30s and subsequently annealed on a hotplate at 80 °C for 10 min in ambient air. A blend of poly[N-9″-hepta-decanyl-2,7-carbazole-alt-5,5-(4′,7′-di-2-thienyl-2′,1′,3′-benzothiadiazole)] (PCDTBT) (1-Material, Inc.) and [6,6]-phenyl C_{70}-butyric acid methyl ester (PCBM70) (Nano-C, Inc.) (35 mg/ml, 1:4 by weight, dissolved in dichlorobenzene) was spin-cast at 1100 rpm for 60 s in an N_2-filled glove box. The film was dried for 1 h in the glove box and annealed on a hotplate at 80°C for 10 min. The fabrication of the samples were finished by depositing TiO_x/Al or MoO_x/Al, depending on the architecture. Table 1 summarizes the initial performance of all the cells that are mentioned throughout the text.

Current density-voltage (J–V) characteristics were measured with a source-measure unit (Keithley 238) under AM 1.5G illumination. The irradiance of the solar simulator (ABET technologies) was checked periodically using a calibrated Si photodiode.

The degradation characteristics were carefully monitored for each cell type and were analyzed using various spectroscopic tools including ultraviolet photoelectron spectroscopy (UPS), X-ray photoelectron spectroscopy (XPS) and optical microscopy.

3. Result and discussion

3.1. Stability test on normal and inverted OSCs with aluminum top electrodes

Fig. 2 presents the evolution in the efficiencies of the normal and inverted OSCs under the specified damp conditions. The open and filled symbols with the same shapes in Fig. 2 correspond to the data obtained from the same batch of normal and inverted OSCs, respectively. (Data obtained from 93 samples in 18 batches for the normal OSC and 64 samples in 15 batches for the inverted OSC are also presented in Fig. S1 in the Supporting information) It can be clearly seen that the inverted OSCs outlive the normal OSCs despite some spread; the efficiency of the normal OSCs decreased rapidly and became negligible in a short amount of time while that of the inverted OSCs decreased abruptly at the beginning but then saturated or slowed its further reduction. Remarkably, in an experiment in which the test was conducted for an extended

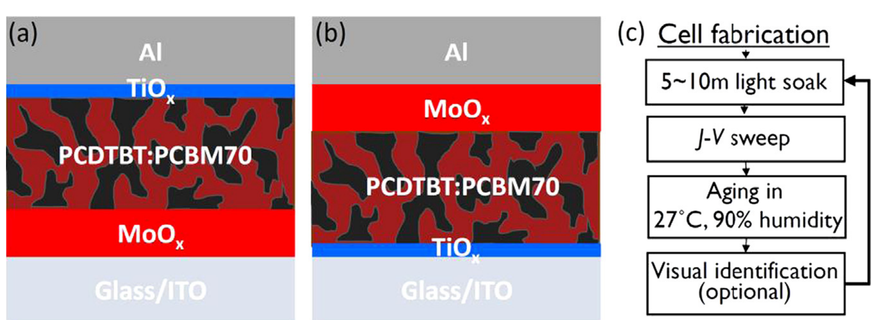

Fig. 1. Device structure of the (a) normal and (b) inverted OSCs, and (c) the cell evaluation sequence.

Table 1
Summary of the initial device performances studied in this work.

		V_{oc} (V)	J_{sc} (mA/cm^2)	FF	PCE (%)
Al top[a]	Normal	0.881 ± 0.092	9.10 ± 1.07	0.57 ± 0.06	4.6 ± 0.53
	Inverted	0.897 ± 0.008	10.01 ± 1.74	0.56 ± 0.02	5.13 ± 0.22
TiO_x anneal (normal)	Pristine	0.825	9.43	0.57	4.46
	Annealed	0.923	8.51	0.53	4.17
MoO_x anneal (inverted)	Pristine	0.892	9.43	0.57	4.79
	Annealed	0.892	9.52	0.56	4.75
MoO_x and TiO_x anneal (inverted)	MoO_x only	0.91	9.88	0.55	5
	Both	0.937	9.64	0.55	5.01

[a] Performance averaged among 106 normal OSCs and 136 inverted OSCs. The values after " ± " represent the standard deviations.